CLM-P772

CLM-P772

UKAEA

Preprint

DEVELOPMENT OF HIGH MANGANESE HIGH NITROGEN LOW ACTIVATION AUSTENITIC STAINLESS STEELS

A. H. BOTT
F. B. PICKERING
G. J. BUTTERWORTH

CULHAM LABORATORY
Abingdon, Oxfordshire
1985

CLM-P772

DEVELOPMENT OF HIGH MANGANESE HIGH NITROGEN LOW ACTIVATION AUSTENITIC STAINLESS STEELS

A.H. Bott*, F.B. Pickering* and G.J. Butterworth**

*Sheffield City Polytechnic, Pond Street, Sheffield, U.K.
**Culham Laboratory, Abingdon, Oxon., OX14 3DB, U.K.
(Euratom/UKAEA Fusion Association)

Abstract

Elementally-substituted high Mn, high N steels have been studied as potential low-activation replacements for austenitic stainless steels of the types AISI 316, 320, 321 and FV548. The approach to the metallurgical design of the compositions and prediction of the basic properties is outlined. Experimental casts of the proposed alloys were prepared and their microstructural constitution, stability and basic mechanical properties investigated. The stability against martensitic transformations under deformation and refrigeration was examined. Ageing at 400°, 650° and 900°C following solution treatment at 1150°C resulted in a fine grain boundary precipitation of TaC accompanied by intragranular and, in some cases, limited σ and Laves phase precipitation. Proof stress values of 470-610 MPa and tensile strengths of 750-1000 MPa were obtained and a high tensile ductility was observed. Fatigue resistance appeared to be similar to that of the established steels but the creep rupture strength was lower than expected.

(Paper for presentation at ICFRM-2, Chicago, 14-17 April 1986)

March 1986

1. Introduction

In order to exploit the potential environmental advantages of thermonuclear fusion with respect to radioactive waste generation, it is desirable to recycle radiation-damaged structural materials after relatively brief storage. Calculations have quantified the acceptability of the chemical elements in terms of the concentrations permitted in a first wall or blanket material such that the post-service contact γ-dose rate would not exceed 2.5×10^{-5} Svh^{-1}, a value at which essentially unrestricted handling could be considered, following a decay period of 100y [1]. Application of this criterion eliminates many of the alloying elements at the concentrations commonly used in high strength steels and in particular Ni, Ti, Mo, Nb and Zr.

This study examines the possibility of developing low-activity stainless steels as alternatives to the well-established austenitic grades AISI 316, 320 and 321 and Firth-Vickers FV548. The design of these replacement alloys is considered on the basis of extrapolations from existing data in order to obtain constitutions, phase stability and transformations and mechanical properties close to those of the conventional steels. Because of the need to extrapolate from existing data, the alternative compositions have been maintained close to those of the original steels, for which a relatively large body of information is available.

Following the metallurgical design phase, experimental casts were made of the proposed alloy compositions and their microstructures, phase stability and mechanical properties determined in order to test the validity of the design concepts.

2. Metallurgical design of the replacement steels

The compositions of the well-established reference austenitic steels are given in Table 1. Since the elements Ni, Mo, Ti and Nb are unacceptable at concentrations exceeding 0.1, 0.2, 0.2 and 0.002%, respectively, it was decided to replace Ni by Mn-C-N combinations, Mo by W, and Ti and Nb by Ta. The first priority was to ensure that the alloys would be fully austenitic after solution treatment at about 1050°C. The constitution of stainless steels at room temperature after cooling from high temperatures can be predicted by means of a Schaeffler-type diagram [2,3] in conjunction with chromium and nickel equivalent values for the principal alloying elements. The following equations for the Cr and Ni equivalents have been successfully applied to a wide range of austenitic steels [4]:

$$\text{Cr equivalent} = (Cr) + 2(Si) + 1.5(Mo) + 5(V) + 5.5(A\ell) + 1.75(Nb) + 1.5(Ti) + 0.75(W) \quad (1)$$

$$\text{Ni equivalent} = (Ni) + (Co) + 0.5(Mn) + 0.3(Cu) + 30(C) + 25(N) \quad (2)$$

where ( ) = mass percent of the element in solution.

Application of these equations must take into account the removal of species from solution as carbides or nitrides, which can be estimated from the appropriate solubility relations.

It was proposed that the Ti and Nb contents of the original steels be replaced by Ta. Tantalum was chosen rather than hafnium on the grounds that the extrapolation to TaC of known solubility data [4,5] for NbC would be less uncertain in view of the closer similarity between TaC and NbC and the corresponding nitrides than between the carbides and nitrides of Hf and Nb, in terms of their crystal structures and heats of formation [6]. In the conventional steels the solubility of NbC increases with the nickel content and, since nickel is to be replaced by Mn-C-N combinations, the influence of Mn on the solubility must be considered. It is known that in low alloy steels Mn increases the solubility of carbides and nitrides. In the absence of definitive data it was assumed that the solubilities of the carbides and nitrides of Ta could be roughly approximated to those of Nb and that the effect of the Mn concentration would be similar to that of Ni.

It was suggested that molybdenum should be replaced by tungsten rather than by vanadium because, whilst the Cr equivalent of V is known, none of the well-characterised commercial steels contain V and so its effect on properties could not readily be predicted. Moreover, it appeared from considerations of the electron vacancy number that V would show an even greater propensity than Cr for the formation of intermetallic compounds [7] and thus enhance any susceptibility to embrittlement should sigma-type phases precipitate during service.

The extent to which nickel can be replaced by manganese alone is limited by the low value (0.5) of the Ni equivalent for Mn. An upper limit of 15% Mn was imposed since there is information in the literature [2] on high strength austenitic steels with Mn contents up to this level and also because there is evidence that at concentrations above 12%, Mn begins to lose its austenite stabilising power. Even at 15%, however, Mn does not completely fulfil the austenite stabilising role of the Ni in the conventional steels and so must be augmented by more potent austenitising elements such as C or N. Of the two, N

seemed preferable on account of its greater solubility in the presence of high Mn concentrations and because an increased carbon content could lead to carbide precipitation and a consequent risk of embrittlement and reduced corrosion resistance. In addition there is information on steels containing at least 15% Mn and 0.5% N [2].

On the basis of the foregoing considerations, low-carbon steels containing up to 19% Cr, 15% Mn and 0.45% N, with additions of up to 5% W and 1.5% Ta were designed with Ni and Cr equivalent values similar to those of the established steels they were to replace. Whilst it was believed that up to 1% Si might be accommodated in the replacement steels it was intended to restrict the Si content to 0.2% in view of its strong ferrite-forming tendency and of its effect in promoting the formation of intermetallic phases [7]. Suggested composition ranges for the replacement alloys and for an alloy designated OPTSTAB, designed to have optimum austenite stability, are given in Table 1. In arriving at the proposed composition ranges the most difficult problem was the assessment of the required Ta content. This was performed by taking the maximum carbon content for the appropriate reference steel and assuming that the Ta would form a phase Ta(C,N) in which C and N were present in equal proportion. From the calculated Ta content it could also be predicted, assuming the solubility of Ta(C,N) to be similar to that of NbC, that at the operating temperature of the first wall or blanket only small concentrations of Ta and (C+N), e.g. 30-70 ppm Ta and 2-5 ppm (C+N), of that available for precipitation would remain dissolved in the austenite. It is also seen that the proposed substitute for 316 steel contains some Ta; this is to prevent loss of corrosion resistance.

3. Predicted metallurgical characteristics of the replacement alloys

It was possible, on the basis of published data, to predict some of the relevant metallurgical characteristics of the alternative alloys, as described below.

3.1 Constitution

The compositional ranges of commercial stainless steels yield Ni and Cr equivalents which, when plotted on the conventional Schaeffler diagram, indicate that a fully austenitic structure is not maintained over the whole range of composition, as illustrated by Fig.1. Several of the compositions would be predicted to contain varying proportions of delta ferrite and some should also undergo partial transformation of the austenite to martensite. The above observations should also apply to the replacement alloys since they are designed to have the same

ranges of Ni and Cr equivalents as their conventional counterparts. It is seen from Fig.1 that a fully austenitic structure would be expected only for compositions lying toward high Ni equivalent and low Cr equivalent values in the proposed composition ranges.

3.2 Phase stability

The instability of austenite can be manifested in two ways, namely a partial transformation to α' martensite on cooling to sub-zero temperatures or during cold deformation at temperatures below M_d, and by the precipitation of δ ferrite or intermetallic compounds at elevated temperatures in the range 500-800°C.

The propensity for martensite formation can be indicated by the M_s temperature of the austenite, which may be calculated from the relation

$$M_s(°C) = 502 - 810(C) - 1230(N) - 13(Mn) - 30(Ni) - 12(Cr) - 54(Cu) - 46(Mo) \quad (3)$$

where ( ) is the mass percent of the alloying element dissolved in the austenite [2]. The average M_s values for the composition ranges of the replacement alloys and the parent steels are given in Table 2. It is seen that, of the conventional steels, type 321 would be the least stable against martensite formation at low temperatures, FV548 being in turn less stable than 316 or 320. The low-activity compositions all have similar M_s values and their susceptibilities to low temperature martensitic transformation would be predicted to lie between those of type 316 and FV548 steels. The tendency of an alloy to form martensite during deformation can be measured by the parameter Md_{30}^{50}, which represents the temperature at which 50% by volume of martensite is formed under a true strain of 0.30. The following equation has been used to predict this Md temperature for austenitic stainless steels [8].

$$Md_{30}^{50}(°C) = 497 - 462(C + N) - 9.2(Si) - 8.1(Mn) - 13.7(Cr) - 20(Ni) - 18.5(Mo) \quad (4)$$

According to this equation, as shown by Table 2, the substituted alloys are likely to form greater amounts of martensite than the standard alloys under deformation; this property may be beneficial to their stretch formability.

The susceptibility to form intermetallic phases of the sigma type during ageing may be predicted from available data on the electron vacancy numbers N_v [7,9]. Whilst the data are mainly applicable to superalloys they can also be applied to stainless steels and a typical equation for N_v is:

$$N_v = 10.66(Nb) + 6.66(Si + Zr) + 5.66(V) + 4.66(Cr + Mo + W) + 3.66(Mn) + 2.66(Fe) + 1.71(Co) + 0.61(Ni) \quad (5)$$

It is usually predicted that sigma-type phases are likely to form with $N_v > 2.5$. From the calculated values given in Table 2 it is seen that, while both the conventional and the replacement alloys are expected to form sigma-type phases, with consequent embrittling effects, the replacement alloys would be more susceptible, largely on account of their high Mn content. The kinetics of the sigma phase precipitation are also important, however, and in fully austenitic structures sigma is known to form extremely slowly such that at operating temperatures around 500°C appreciable precipitation may not occur in less than about 10^5h. The process may well be accelerated during irradiation, though this effect cannot be quantitatively predicted.

3.3 Stacking fault energy

A low stacking fault energy (SFE) increases the work hardening rate, resulting in high forming loads and a greater tensile strength relative to the proof stress. If the work hardening rate is high relative to the flow stress, however, there will be a high uniform strain prior to plastic instability and hence an enhanced stretch formability [2]. A low SFE will, moreover, increase the tendency to ε martensite formation, particularly during straining, and because ε martensite may be a precursor to α' martensite formation [10] it will also tend to increase the susceptibility to strain-induced martensitic transformation, indicated by an increased Md temperature. This effect can also lead to improved stretch formability if there is a critical proportion of α' martensite formed at strains of about 0.2 [2,11].
A predictive relationship exists for calculation of the SFE of austenitic stainless steels [12] and this may be extrapolated to predict the SFE of the replacement alloys. In any case only relative, rather than absolute, values can be obtained. Calculations indicate that 321 has the lowest SFE of the conventional steels and this is consistent with its high M_s and Md temperatures. The substituted steels are predicted to have much lower SFE and again 321T has the lowest calculated value. On the basis of the SFE values it would be anticipated that the low activation steels would have higher work hardening rates, higher tensile strengths and a greater propensity for

deformation-induced martensite formation than the standard steels. The replacement steels should therefore exhibit at least equivalent and probably superior stretch forming properties compared with their commercial analogues.

3.4 Strength

The following equations given in the published literature [2] were used to estimate the 0.2% proof stress and tensile strength values:

$$\text{0.2\% Proof stress (MPa)} = 68 + 354(C) + 20(Si) + 4(Cr) + 14(Mo) + 18(V) + 4(W) + 26(Ti) + 12(A\ell) + 493(N) + 7.1d^{-\frac{1}{2}} \quad (6)$$

$$\text{Tensile strength (MPa)} = 447 + 539(C) + 847(N) + 37(Si) + 2(Ni) + 18(Mo) + 77(Nb) + 46(Ti) + 18(A\ell) + 12.7d^{-\frac{1}{2}} \quad (7)$$

where d is the mean austenite grain size in mm.

In employing these equations the effect of any delta ferrite was excluded, as a fully austenitic structure was assumed, and a value of d corresponding to a grain size of ASTM 5 was used. It is also necessary to extrapolate the equations beyond the nitrogen contents for which they were derived and to neglect any solid solution hardening factor for Mn, which in conventional steels varies only over a limited range. Consequently, the calculated strength values of the substituted alloys, which are compared with those of the original steels in Table 2, can serve only as a rough indication. The values given in Table 2 are averages over the proposed composition ranges. It is seen from the table that the replacement alloys would be expected to have substantially higher proof stress and tensile strength values and, in particular, a greater difference between proof stress and tensile strength. The latter result suggests that the replacement alloys should have higher work hardening rates than the conventional steels.

3.5 Creep properties

Although thermal creep is an important property in elevated temperature application there appears to be little quantitative data on which to base predictions. An empirical equation has been proposed for the rupture life of Nb-bearing type 347 steel [5] for a stress of 185 MPa at 700°C:

$$\ell n\ t_r = (2.4 \pm 2.7) + (7.7 \pm 2.2)(NbC_{ppt}) + (1.24 \pm 0.47)\ NbC_u \quad (8)$$

where t_r = rupture life in hours, NbC_{ppt} is the volume fraction of NbC precipitated during the rupture test and NbC_u the volume fraction of undissolved NbC. On the assumption that Ta(C,N) in the substituted alloys behaves similarly to NbC in type 347 steel, equation (8) would predict a rupture life of a few hundred hours. This rather low value may signify the limited applicability of the predictive equation to alloys in the fully prior aged condition.

3.6 Void swelling

Austenitic stainless steels can undergo substantial volume increases as a consequence of irradiation induced void swelling, the detailed swelling behaviour depending on the nature of the radiation, temperature, alloy composition and degree of cold work. The void swelling of Fe-Ni-Cr alloys and austenitic stainless steels has been correlated with the electron vacancy number N_v [4,13] and appears to increase rapidly for $N_v > 2.5$. This behaviour has been attributed to the onset of structural changes, in particular, sigma precipitation. If this can be used as a basis for prediction of void swelling in the replacement steels then their N_v numbers would indicate them to have less swelling resistance than the standard steels. The swelling behaviour must be established by experiment but it may be anticipated that the substitute steels will not exhibit swelling very different from that of the conventional grades. It has, however, been demonstrated that high Mn, high N alloys swell less than conventional steels [14].

4. Experimental evaluation of the proposed LA alloys

An investigation of the structures and properties of the five alloys 316T, 320T, 321T, FV548T and OPTSTAB, prepared in accordance with the proposed low activity compositions, was performed to validate the metallurgical design and property predictions. The alloys were manufactured as 10kg vacuum melts using high-purity raw materials, the ingots being surface dressed and hot rolled to 20 mm thick plate in 4 passes with interpass reheating at 1150°C. The actual compositions are shown in Table 1, high Mn and N contents being chosen for 320T and 321T in an attempt to ensure a fully austenitic structure and the Si contents of all the steels being kept below 0.2%.

4.1 Constitution

Specimens were solution treated at 1000-1250°C for 30 minutes and then water quenched. Figure 2 shows the measured delta ferrite

contents as a function of solution treatment temperature. Alloys 320T and OPTSTAB were fully austenitic over the whole range 1000-1250°C whilst 321T contained only 10% delta ferrite at 1200°C and was fully austenitic at all other temperatures. Alloys 316T and FV548T were fully austenitic up to 1050°C but at temperatures from 1100° to 1250°C showed increasing delta ferrite contents, a feature expected of alloys that are not fully austenitic.

According to the standard Schaeffler diagram, all the alloys should have been fully austenitic, as shown by Fig.3, while a Schaeffler diagram developed specifically for Cr-Mn steels [16] indicated even greater stability of the austenitic constitution. It is therefore concluded that the Schaeffler type diagrams consistently overestimate the austenitising power of Mn or N, or alternatively underestimate the ferrite forming action of W and Ta in these Cr-Mn-N base steels.

4.2 Effects of ageing

After solution treatment at 1150°C specimens of each alloy were aged for times up to 1000h at 400°C, 650°C and 900°C while the progress of ageing was followed by hardness measurements and microstructural examinations. The initial hardness was found to be strongly dependent on the N content, in spite of the fact that alloys 316T and FV548T contained 10-15% delta ferrite, thus confirming the very strong solid solution hardening action of N. All the alloys gave similar ageing curves, typified by that for OPTSTAB shown in Fig.4.

At 400°C age hardening started after about 100h and continued at a low rate with increasing time. The hardening was found to be associated with a small degree of $M_{23}C_6$ precipitation and increased generally with higher C contents. Ageing at 650°C gave the expected increase in both the degree and rate of age hardening in all the alloys and was associated with Ta(C,N) precipitation. As would be expected in these hypostoichiometric compositions, the hardening was intensified with higher Ta content. During ageing at 650°C of 316T and FV548T, which contained delta ferrite, transformation of the ferrite to sigma phase commenced after 100h and reached 10% and 9% sigma, respectively, after 1000h. This observation accords with the known acceleration of sigma generation from delta ferrite [17] and it is significant that the fully austenitic alloys were completely resistant to sigma formation in times up to 1000h at 650°C. Moreover, a phase having a needle-like morphology was observed in 316T and FV548T; this was shown by EDX to contain Ta and Fe, suggestive of Laves phase. Ageing at 900°C induced a marked increase in hardness of all the alloys

even after 1h and overaging was progressive with time beyond 10h. The effect was found to be associated with the precipitation of Ta(C,N), which coarsened with time. No sigma phase was observed during ageing at 900°C but some Laves phase Fe_2Ta was seen in alloys 316T and FV548T and this phase progressively spheroidised with increasing ageing time.

4.3 Transformation to martensite

The tendency of the alloys to transform to martensite under cold deformation and under refrigeration was studied. Transmission electron microscopy of specimens 10% cold worked at 20°C revealed similar structures for all the substitution alloys and these comprised deformation twins, ε martensite and stacking faults, as shown by Fig.5a. It was not possible to determine unambiguously the proportions of the different structures since this is generally difficult [10] and, as ε martensite nucleates from overlapping stacking faults, the transition from one to another is indistinct. More ε martensite/stacking faults were observed in the 316T and 320T steels, as would be expected from the calculated SFE of the alloys. Since the relationships used to predict the susceptibility to deformation-induced martensite transformation apply to α' rather than to ε martensite, it is unlikely that they can predict the tendency for formation of the latter, though it is suggested that greater degrees of cold work than the 10% employed here might well produce α' martensite in view of the pre-existing ε martensite which is known to act as a nucleating agent for α' martensite.

In all the replacement alloys refrigeration to -196°C resulted in structures containing both α' and ε martensite, as illustrated by Fig.5b. It was evident that alloys 316T, FV548T and OPTSTAB contained more α' martensite than did the alloys 320T and 321T, in agreement with their calculated M_s temperatures based on their chemical compositions.

4.4 Tensile properties

The tensile properties of the alloys solution treated at 1150°C were measured at 20°C and at 500°C, the results being presented in Table 3.

4.4.1 Room temperature properties

The 0.2% proof stress and tensile strength values of the substitute alloys were found to be considerably higher than those of the original steels and, with the sole exception of the tensile strength of 321T as illustrated by Fig.6, the observed values were also

appreciably higher than the values calculated from equations (6) and (7). The results suggest that the predictive equations underestimate the solid solution hardening effects of W, Ta and especially of N, and perhaps indicate the invalidity of extrapolating the equations beyond the compositional range for which they were established. It can also be seen that the equations are more successful at predicting the tensile strength than the proof stress. The relatively low tensile strength of alloy 321T may be associated with its low W and Ta contents.

The work hardening rate of the replacement steels is much higher than that for the established steels [2] and there is a clear tendency, as would be expected, for the rate to increase with decreasing calculated relative SFE, as shown by Fig.7. This figure also confirms the expected result that the maximum uniform elongation increases with the work hardening rate and points to a high stretch formability. The tensile ductility values of the substituted alloys are generally satisfactory and possibly superior to those of the conventional steels. From their room temperature tensile properties the replacement alloys, particularly OPTSTAB, are expected to exhibit a greater stretch formability, though the high proof stress values will result in high flow stresses and thus high forming loads.

4.4.2 Tensile properties at 500°C

The tensile properties measured at 500°C are listed in Table 3. The proof stress values are approximately twice those of the conventional steels [18], indicating an adequate retention of strength. Tensile strengths in the range 520-617 MPa are observed, as compared with 400-450 MPa for AISI 316 and 321 steels [18]. The general ductilities at 500°C appear adequate and the ratios of the proof stress values at 20°C and 500°C average 1.93 whilst those of the tensile strengths average 1.55.

4.5 Creep properties

Accelerated creep rupture tests were performed in air at 700°C, which is above the anticipated operating temperature, under a stress of 185 MPa. As noted in section 3.5 the rupture life was estimated to be a few hundred hours while, as shown by Table 2, the observed rupture lives ranged from 190 to 420h. It is noteworthy that the two replacement alloys containing the highest Ta contents, namely 316T and FV548T, had the longest rupture lives. This feature is understandable since all the alloys contain less than the stoichiometric content of Ta for formation of Ta(C,N) and those with highest Ta content are closest

to stoichiometry. It is known that alloys of stoichiometric composition have the strongest temperature dependence of solubility and hence the greatest degree of carbide precipitation during elevated temperature exposure, such that the rupture life is maximised [5]. On the assumption that Ta(C,N) behaves similarly to NbC in type 347 steel it would be expected that an alloy with stoichiometric Ta:(C+N) ratio would give a rupture life of about 10^3h under the present conditions [5]. Consequently it is suggested that improved creep rupture properties would be obtained on increasing the Ta:(C+N) ratio to stoichiometry and also by increasing both Ta and (C+N) contents in this ratio so that more undissolved Ta(C,N) is produced at the solution treatment temperature.

4.6 Fatigue properties

Since reactor structures would be subject to thermal and mechanical stress cycling a preliminary assessment of the fatigue properties of the substituted alloys was made. Compact tension specimens measuring 31.25 x 30 x 12.5 mm with a notch depth of 12.5 mm were pre-fatigued to provide an initial notch of constant acuity and then tested by cycling with a constant amplitude triangular waveform for load reversals at a maximum load of 200kN and a frequency of 10Hz. The observed number of cycles to failure at room temperature are presented in Table 2 as a percentage of the number of cycles to failure of AISI 316 steel tested under identical conditions. The fatigue lives of the experimental alloys all lie within 84-126% of that for AISI 316, indicating that they should exhibit general fatigue properties similar to those of the standard compositions.

4.7 Manganese depletion

It has been reported that the loss of manganese by evaporation from the surface of high Mn steels can reduce the austenite stability [6,15]. To investigate whether this was the case for the replacement alloys, specimens of 320T and OPTSTAB, representing the highest and lowest Mn contents, were heated at 650°C for 10^3 hours under a vacuum of 10^{-4} torr. Subsequent EDX examination showed that, for both alloys, manganese loss was confined to a layer extending 0.01 mm from the surface. The maximum depletion amounted to 1.5%, which would not normally reduce the Mn content below the lower specification limit. It is therefore believed that volatilisation of Mn would not materially destabilise the overall microstructure of the substituted alloys.

5. Conclusions

The following conclusions have been drawn from these studies:

1. The proposed low-activation alloys could be fabricated satisfactorily and suffered no detrimental effects during hot rolling. There was no apparent deterioration in hot workability.

2. All the alloys were fully austenitic up to 1050°C though the usual Schaeffler diagram and values for Ni and Cr equivalent coefficients appeared to overestimate the stability with respect to delta ferrite formation. A modified Schaeffler diagram determined specifically for Cr-Mn austenitic steels proved even less reliable in this respect.

3. Material solution treated at 1150°C showed little precipitation hardening up to 10^3h at 400°C but more rapid and intense hardening at 650°C and 900°C, with overaging after more than 1h at 900°C. Small proportions of $M_{23}C_6$ were formed at 400°C, Ta(C,N) being precipitated at 650°C and 900°C. Precipitation hardening at 650°C was more pronounced with the higher Ta contents. Laves phase, based on Fe_2Ta, was precipitated at 900°C and spheroidised at long ageing times. Sigma phase formed only after 100h at 650°C but not even after 1000h at either 400° or 900°C. Moreover, sigma formation was observed only in the alloys containing delta ferrite, the fully austenitic alloys being resistant to sigma formation up to at least 10^3h at 400°, 650° or 900°C.

4. Cold working to 10% at 20°C led to generation of deformation twins, stacking faults and ε martensite to an extent that reflected the calculated SFE of the alloys. Refrigeration at -196°C caused partial transformation of the austenite to α' and ε martensite to a degree which related to the calculated M_s temperatures.

5. The room temperature tensile strength and 0.2% proof strength appreciably exceed those of conventional austenitic stainless steels, the observed values being considerably greater than those estimated from relationships established for commercial steels. The work hardening rate followed the trends indicated by the calculated SFE and a close relationship was found between the maximum uniform elongation and the observed work hardening rate. The general ductility values were at least equal to those of

conventional steels. Room temperature tensile properties indicate that the formability of the replacement alloys is probably superior to that of conventional steels, at least with respect to stretch forming, though forming loads will be higher.

6. The tensile properties in terms of both strength and ductility at 500°C are at least equivalent to those of the conventional grades.

7. The creep rupture lives were found to be about as predicted from equations derived for stainless steels containing Nb but lower than for type 347 steel tested under the same conditions. Possible reasons for the difference have been suggested and ways of improving the creep properties indicated.

8. The fatigue properties appear to be similar to those of AISI 316 steel.

9. Exposure of the alloys at 650°C for 10^3h under a vacuum of 10^{-4} torr was found to cause a Mn depletion of about 1.5% from a surface layer of thickness not exceeding 0.01 mm. It is concluded that this Mn loss would not materially destabilise the austenite.

10. Finally, the experimental study has generally confirmed the validity of the approach adopted for the metallurgical design of replacement low-activation alloys and has indicated that their properties should in general be at least equivalent, in the aspects investigated, to those of the conventional steels they were designed to replace.

References

[1] O.N. Jarvis, Harwell Report AERE-R 10860, 1983.

[2] F.B. Pickering, Physical Metallurgy and the Design of Steels, Applied Science Publishers, 1978.

[3] H. Schneider, Foundry Trade Journal 108 (1960) 562.

[4] D.R. Harries, Int. Conf. on Mechanical Behaviour and Nuclear Applications of Stainless Steels at Elevated Temperatures, Varese, 20-22 May, 1981.

[5] S.R. Keown and F.B. Pickering, Proc. Conf. 20-22 Sept. 1972, Sheffield, Publ. Met. Soc. 134.

[6] H.J. Goldschmidt, Interstitial Alloys, Butterworths, 1967.

[7] R.F. Decker, Int. Symp. on Strengthening Mechanisms in Steels, Zurich, Climax Molybdenum Co., 1969, p147.

[8] T. Angle, J.I.S.I. 173 (1954) 165.

[9] S.P. Rideout et al., J. of Met. 3 (1951) 872.

[10] M.W. Bowkett and D.R. Harries, Harwell Report AERE-R 9093, 1978.

[11] T. Gladman et al., Sheet Metal Industries 51 (1974) 219.

[12] R.E. Schramm and R.P. Reed, Met. Trans. 6 (1975) 1345.

[13] J. Cawley, PhD Thesis, Sheffield City Polytechnic, 1982.

[14] M. Snykers and E. Ruedl, Proc. 11th Symp. on Fusion Technology, Oxford, 15-19 Sept., 1980.

[15] D.J. Mazey et al., Harwell Report AERE-R 9931, 1980.

[16] E. Ruedl, D. G. Rickerby and T. Sasaki, Proc. 13th Symp. on Fusion Technology, Varese, Sept. 1984.

[17] F.R. Beckitt, JISI 207 (1969) 632.

[18] BSCC High Temperature Data Book. Publ. Iron and Steel Institute, 1973.

Table 1 Composition ranges of the conventional and proposed replacement stainless steels. Values in brackets indicate the actual compositions of the experimental casts.

Alloy type	Composition in mass percent (balance Fe)												equivalent values	
	C	Mn	Si	Ni	Cr	Mo	W	Ti	Nb	Ta	N	B	Cr	Ni
316 conventional	0.03–0.06	2 max	1 max	10.0–14.0	16.0–18.0	2.0–3.0	–	–	–	–	0.02 max	–	19.0–24.5	10.0–15.0
316 replacement (316T)	0.03–0.06 (0.038)	10.0–14.5 (14.5)	1 max (0.17)	– –	16.0–18.0 (16.3)	–	4.0–6.0 (4.10)	–	–	0.8–1.6 (1.35)	0.23–0.36 (0.259)	– –		
320 conventional	0.06 max	2 max	1 max	10.0–14.0	16.0–19.0	2.0–3.0	–	0.3 min	–	–	0.02 max	–	19.0–25.5	10.0–15.0
320 replacement (320T)	0.06 max (0.050)	10.0–14.5 (14.8)	1 max (0.18)	– –	16.0–19.0 (17.7)	– –	4.0–6.0 (4.22)	– –	– –	1.6 max (0.76)	0.20–0.36 (0.415)	– –		
321 conventional	0.08 max	2 max	1 max	9.0–12.0	17.0–19.0	–	–	0.4 min	–	–	0.02 max	–	17.5–21.8	9.0–13.0
321 replacement (321T)	0.08 max (0.060)	8.0–11.5 (11.9)	1 max (0.16)	– –	17.0–19.0 (17.6)	– –	0.7–1.1 (1.00)	– –	– –	2.4 max (0.68)	0.20–0.36 (0.432)	– –		
FV548 conventional	0.06–0.09	2 max	0.6 max	11.0–12.0	16.0–17.0	1.00–1.75	–	0.005 max	1.05 max	–	–	0.001–0.003	17.5–21.7	11.0–13.0
FV548 replacement (FV548T)	0.06–0.09 (0.053)	11.0–13.0 (12.3)	0.6 max (0.17)	– –	16.0–17.0 (16.4)	– –	2.0–3.5 (2.20)	– –	– –	1.7–2.7 (1.50)	0.26–0.36 (0.269)	– –		
OPTSTAB	0.08 max (0.070)	10.0–12.0 (11.9)	1 max (0.19)	– –	14.0–16.0 (14.2)	– –	1.5–2.5 (2.15)	– –	– –	1.5 max (0.50)	0.22–0.36 (0.285)	– –	15.1–20.1	10.0–14.0

Table 2 Table showing predicted transformation temperatures, electron vacancy numbers and tensile strengths for all the alloys and the measured rupture and fatigue lives of the tailored alloys. The predicted values are averages for the compositional ranges.

Alloy type	Predicted Ms temperature (°C)	Predicted M_{d30}^{50} temperature (°C)	Calculated electron vacancy number (N_v)	Predicted 0.2% proof stress (MPa)	Predicted tensile strength (MPa)	Rupture life at 700°C under 185 MPa stress (h)	Fatigue life as percentage of that of type 316 (%)
316	-190	-35	2.86	177	532		
316T	-175	+42	3.41	289	682	408	124
320	-196	-42	2.83	179	532		
320T	-181	+36	3.44	291	682	284	96
321	-42	+28	2.82	117	484		
321T	-142	+54	3.17	270	662	248	101
FV548	-103	+25	2.82	155	503		
FV548T	-147	+60	3.28	260	662	420	113
OPTSTAB	-154	+83	3.11	276	694	190	84

Table 3 Tensile properties of the substitute alloys at room temperature and 500°C. The work hardening rate is measured at a true strain of 0.2.

Alloy type	Room temperature properties							Properties at 500°C				
	0.2% proof stress (MPa)		tensile strength (MPa)		work hardening rate (MPa)	uniform elong. (%)	total elong. (%)	reduction of area (%)	0.2%PS (MPa)	TS (MPa)	uniform elong. (%)	total elong. (%)	R of A (%)
	obs.	calc.	obs.	calc.									
316T	581	290	807	690	265	31	39	54	301	520	17	22	63
320T	612	375	870	830	420	36	44	53	354	617	31	38	56
321T	512	370	768	850	439	41	49	68	260	551	25	33	72
FV548T	520	290	785	710	397	39	47	60	268	535	22	29	67
OPTSTAB	469	300	1006	735	658	60	62	42	227	525	36	42	62

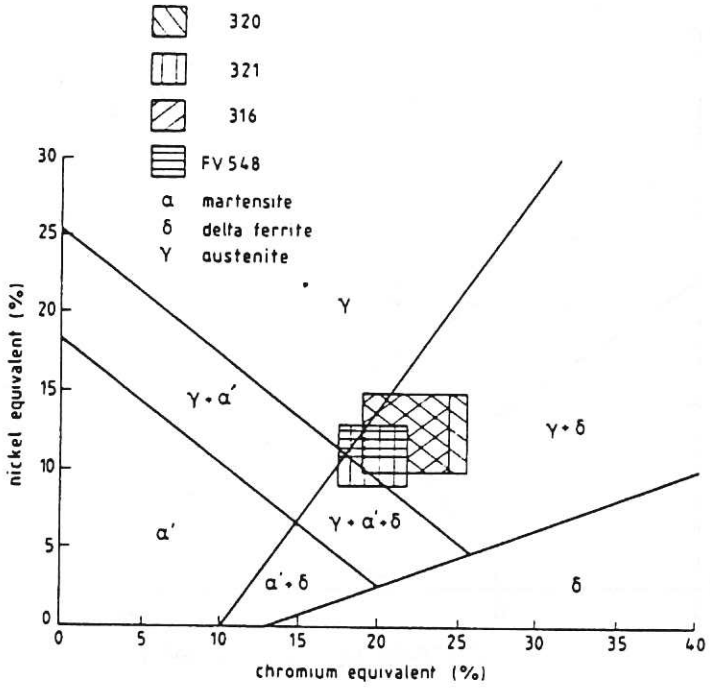

Fig.1 Schaeffler diagram showing the regions representing the conventional and equivalent replacement austenitic stainless steels.

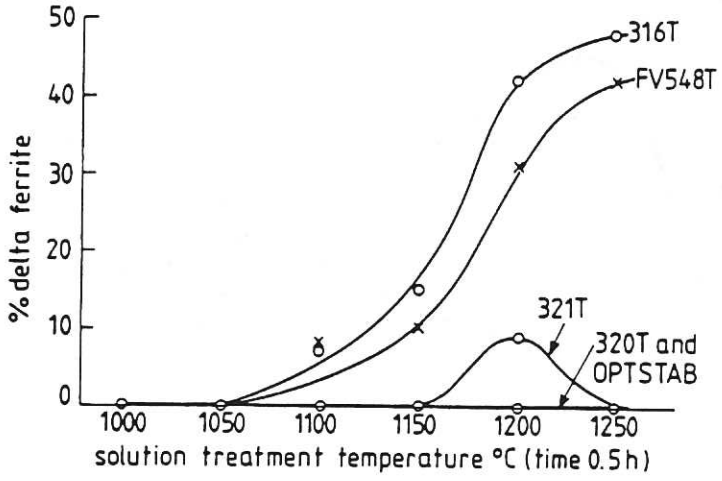

Fig.2 Effect of solution treatment temperature on the constitution of the replacement alloys with respect to delta ferrite content.

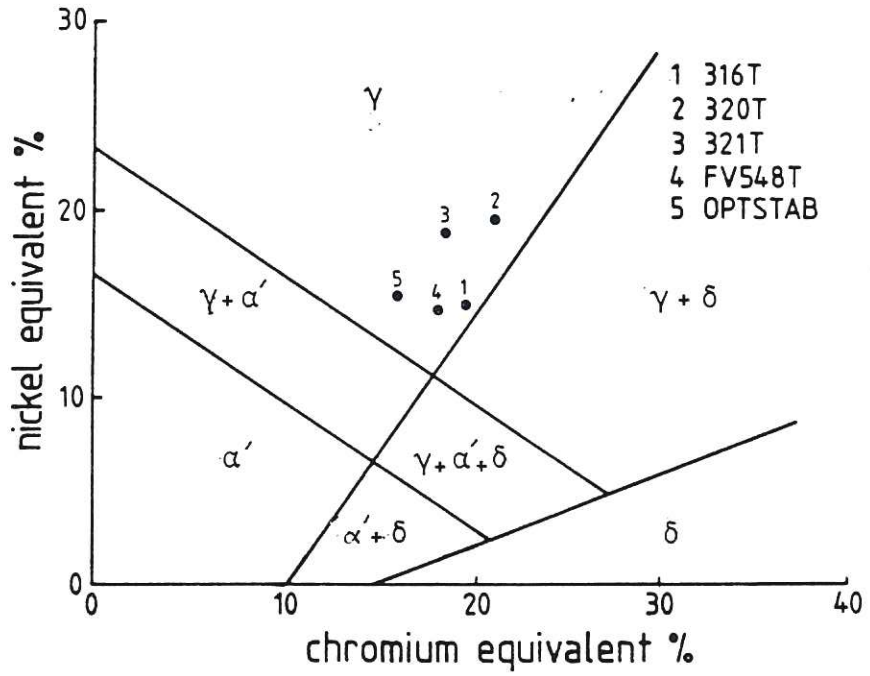

Fig.3 Compositions of experimental casts of replacement alloys plotted on the standard Schäffler diagram.

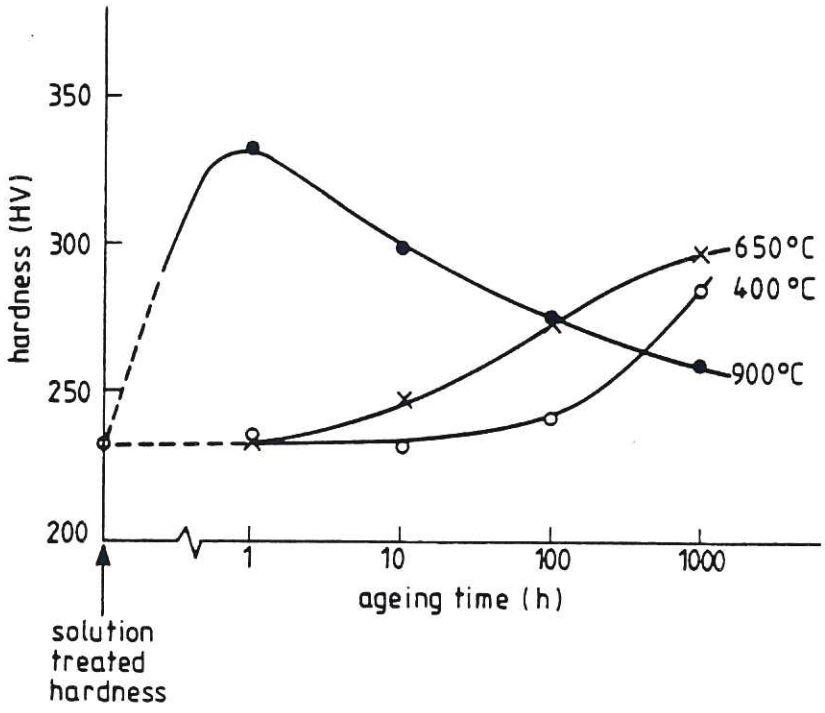

Fig.4 Curves showing age hardening effects in the optimum stability replacement alloy OPTSTAB.

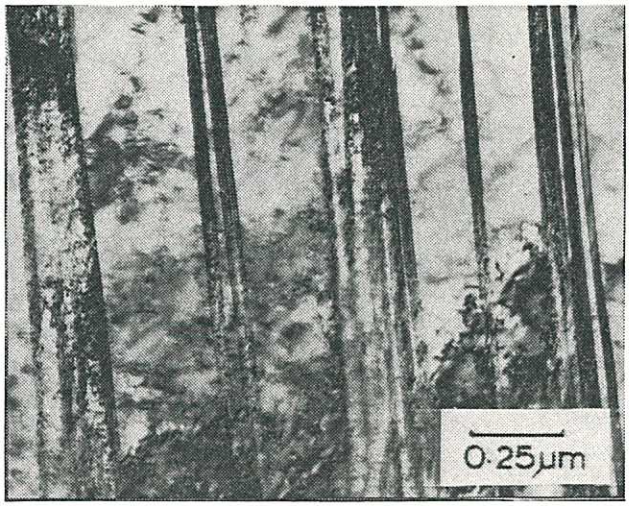

(a) OPTSTAB alloy, magnification 40,000, showing deformation twins, stacking faults and ε martensite.

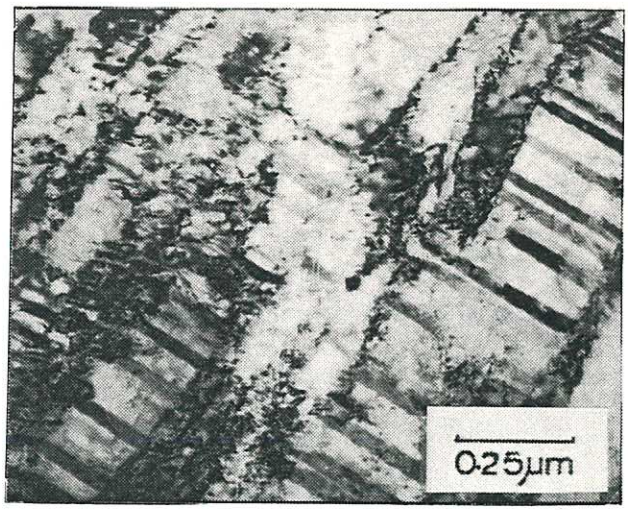

(b) FV548T alloy, magnification 50,000, showing α' martensite with stacking faults or ε martensite between α' laths.

Fig.5 Electron micrographs showing transformation of austenite

(a) after 10% deformation at 20°C.

(b) after refrigeration at - 196°C for 24 h.

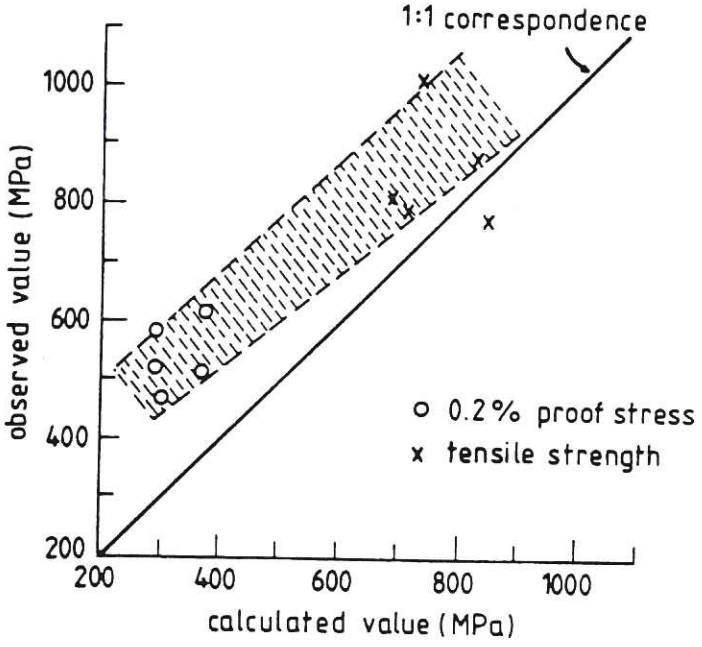

Fig.6 Comparison of calculated and observed proof stress and tensile strength values at 20°C.

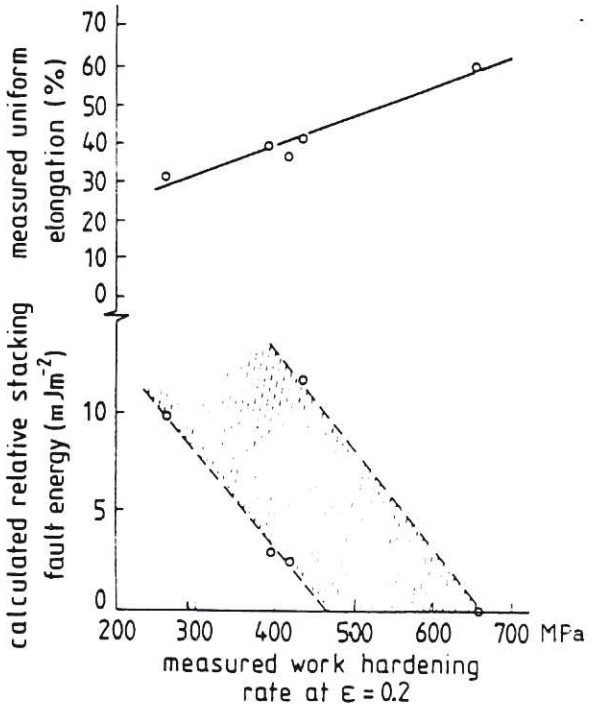

Fig.7 Relationships between the measured work hardening rate, calculated relative stacking fault energy and uniform elongation at 20°C.